NASA Technical Memorandum 106227

High Efficiency Direct Thermal To Electric Energy Conversion From Radioisotope Decay Using Selective Emitters and Spectrally Tuned Solar Cells

Donald L. Chubb and Dennis J. Flood
Lewis Research Center
Cleveland, Ohio

and

Roland A. Lowe
Cleveland State University
Cleveland, Ohio

Prepared for the
Third European Space Power Conference
cosponsored by the European Space Agency and Austrian Space Agency
Graz, Austria, August 23–27, 1993

HIGH EFFICIENCY DIRECT THERMAL TO ELECTRIC ENERGY CONVERSION FROM RADIOSOTOPE DECAY USING SELECTIVE EMITTERS AND SPECTRALLY TUNED SOLAR CELLS

Donald L. Chubb and Dennis J. Flood
National Aeronautics and Space Administration
Lewis Research Center
Cleveland, Ohio 44135

and

Roland A. Lowe
Cleveland State University
Cleveland, Ohio 44115

SUMMARY

Thermophotovoltaic (TPV) systems are attractive possibilities for direct thermal-to-electric energy conversion, but have typically required the use of black body radiators operating at high temperatures. Recent advances in both the understanding and performance of solid rare-earth oxide selective emitters make possible the use of TPV at temperatures as low as 1200K. Both selective emitter and filter system TPV systems are feasible. However, requirements on the filter system are severe in order to attain high efficiency. A thin-film of a rare-earth oxide is one method for producing an efficient, rugged selective emitter. An efficiency of 0.14 and power density of 9.2 W/KG at 1200K is calculated for a hypothetical thin-film neodymia (Nd_2O_3) selective emitter TPV system that uses radioisotope decay as the thermal energy source.

1. INTRODUCTION

Thermophotovoltaic (TPV) energy conversion is an attractive concept for attaining efficient direct conversion at moderate temperatures, (1000 to 1500K) using a radioisotope heat source. In TPV conversion, thermal energy is first converted to radiant energy, which is then converted to electrical energy by a photovoltaic (PV) cell. There are two types of TPV systems, illustrated in figure 1. One system uses a black body like thermal emitter (fig. 1(a)). Since the thermal emitter emits large amounts of radiation at energies that cannot be efficiently converted by the PV cell, a bandpass filter is placed between the emitter and the PV cell. The ideal filter allows all photons with energy near the PV bandgap energy, E_g, to pass from the emitter to the PV cell and reflects all photons with energy greater or less than E_g back to the emitter. In other words, the filter makes the thermal emitter perform like a selective emitter. The other system uses a selective emitter that emits in a narrow energy band just above the PV cell bandgap energy, E_g, where the PV cell is most efficient (fig. 1(b)). There are two major obstacles to the development of an efficient, moderate-temperature selective-emitter TPV system. First, an efficient selective emitter must be developed. Second, a PV cell having a bandgap energy very close to the emission band energy of the selective emitter must also be developed. These problems will be discussed in this paper.

2. FILTER AND SELECTIVE EMITTER TPV SYSTEMS

2.1 Filter System Efficiency

In the filter TPV system, most of the emitted radiation is circulated back and forth between the emitter and filter. Therefore, even a small filter absorptivity, α_f, will result in a major loss. Also, if the thermal emitter does not perform like a black body (emissivity = ϵ_E = absorptivity = $\alpha_E = 1$) the efficiency will be reduced.

Consider the efficiency of a filter TPV system. Referring to figure 1(a), the following energy balance applies to the thermal emitter.

$$P_t + \alpha_E r_f P_{rad} = P_L + P_{rad} \tag{1}$$

Where, r_f is the filter reflectivity and

$$r_f + \alpha_f + \tau_f = 1 \tag{2}$$

where α_f is the filter absorptivity and τ_f is the filter transmittance. Define the emitter thermal efficiency as

$$\eta_{th} = (P_t - P_L)/P_t \tag{3}$$

and also the photovoltaic efficiency as

$$\eta_{PV} = P_{EL}/\tau_f P_{rad} \tag{4}$$

Substituting equations (3) and (4) into (1) yields the following result for the overall efficiency of the filter system.

$$\eta_{Tf} = P_{EL}/P_t = \eta_{th}\, \eta_f\, \eta_{PV} \tag{5}$$

Where the filter efficiency, η_f, is the following.

$$\eta_f = \tau_f/(1 - \alpha_E r_f) = \tau_f/[1 - \alpha_E(1 - \alpha_f - \tau_f)] \tag{6}$$

In reference 1 the transmittance for an ideal filter is derived. An ideal filter transmits only within the narrow photon energy band, ΔE_b. In this case (ref. 1)

$$\tau_f = \tau_g\, F(E_b/kT_E,\, \Delta E_b/E_b) \tag{7}$$

Where, τ_g is the effective filter transmittance in the energy band ΔE_b, E_b is the energy at the center of the band and T_E is the thermal emitter temperature. Also,

$$F(s,t) = 15/\pi^4 \int_{s(1-t/2)}^{s(1+t/2)} x^3/(e^x - 1)\, dx \tag{8}$$

and

$$\tau_g = \tau_b\, \epsilon_b/\epsilon_{th} \tag{9}$$

where τ_b is the filter transmittance within the energy band ΔE_b, ε_b is the emitter emittance within the energy band ΔE_b and ε_{th} is the total emitter emittance.

2.2 Selective Emitters

The early work of White and Schwartz (ref. 2) recognized the benefits of selective emitters for efficient TPV energy conversion. However, finding an efficient selective emitter has been a difficult task. The most promising solid selective emitters have been the rare-earth elements (ref. 3). For doubly and triply charged ions of these elements in crystals, the orbits of the valence 4f electrons, which account for emission and absorption, lie inside the 5s and 5p electron orbits. As a result, the rare-earth ions in the solid state have radiative characteristics much like they would have if they were isolated. They emit in narrow bands rather than in a continuum as do most solids. The 5s and 5p electrons "shield" the 4f valence electrons from the surrounding ions in the crystal.

Early spectral emittance work (ref. 3) on rare-earth oxides suitable for TPV showed strong emission bands. However, the emittance for photon energies below the bandgap for PV materials was also significant. As a result, the efficiency of these emitters was low. In the last few years, however, Nelson and Parent (refs. 4 and 5) have reported a large improvement in rare-earth oxide emitters. Their emitters are constructed of fine (5 to 10 μm) rare-earth oxide fibers similar to the construction of the Welsbach mantle used in gas lanterns. The very small characteristic dimension of the emitter results in low emittance for the low energy part of the spectrum, thus giving a much higher efficiency than previous emitters.

2.2.1 Rare-Earth Oxide Solid Selective Emitter Efficiency

The mantle type emitters of Nelson and Parent (refs. 4 and 5) show a single strong emission band centered around some photon energy, E_b. For photon energies below and above this emission band the emissivity is greatly reduced. Therefore, Chubb (ref. 1) used the following model to describe the rare-earth oxide emitters. There is a single emission band of width ΔE_b, with emissivity, ε_b. Outside the emission band the emissivity is ε_l for $E \leq E_b - \Delta E_b/2$ and ε_u for $E \geq E_b + \Delta E_b/2$. This model applies to the mantle type emitter, as well as the thin film emitter to be discussed later. The emitter radiative efficiency is defined as follows,

$$\eta_E = P_E/P_{rad} \tag{10}$$

where P_E is the emitted radiative power from the emission band at E_b and P_{rad} is the total emitted radiative power. Obviously, this efficiency does not include thermal conductive or convective heat loss (P_L in fig. 1). A PV material with bandgap energy, $E_g \approx E_b$ is capable of efficient conversion of this useful energy, P_E. Chubb (ref. 1) has derived the following expression for η_E.

$$\eta_E = [1 + \varepsilon_l/\varepsilon_g \, G(E_b/kT_E, \Delta E_b/E_b) + \varepsilon_u/\varepsilon_g \, H \, [E_b/kT_E, \Delta E_b/E_b]^{-1} \tag{11}$$

The functions G and H are defined in reference 1 and the wavelength and photon energy are related by $\lambda = hc/E$. As can be seen from equation (11), there are four parameters that determine the efficiency.

2.3 Comparison of Filter and Selective Emitter Efficiencies

Now compare the efficiencies of the filter and selective emitter TPV systems. The overall efficiency of the filter system is given by equation (5). Similarly, referring to figure 1(b), the overall efficiency of the selective emitter system is

$$\eta_{Ts} = \eta_{th}\, \eta_E\, \eta_{PV} \tag{12}$$

If both systems operate in the same energy band, ΔE_b, then η_{PV} will be the same in both systems. Also, η_{th} should be nearly the same in both systems. As a result,

$$\eta_{Tf}/\eta_{Ts} \approx \eta_f/\eta_E \tag{13}$$

so that η_f and η_E determine which system has the higher efficiency.

Figure 2 compares η_E and η_f as functions of E_b/kT_E for several values of the filter absorptivity, α_f, and selective emitter emissivity ratios, $\varepsilon_l/\varepsilon_b = \varepsilon_u/\varepsilon_b$. From Nelson and Parent's result (refs. 4 and 5), $\varepsilon_l/\varepsilon_b$ and $\varepsilon_u/\varepsilon_b$ range from 0.01 to 0.1 and $\Delta E_b/E_b$ ranges from 0.05 to 0.15. Thus $\Delta E_b/E_b = 0.1$ was chosen for both the filter and selective emitter systems. Also, for the filter system it was assumed that the thermal emitter behaves like a black body, so that $\alpha_E = \varepsilon_E = 1.0$. Therefore, the filter system is assumed to have an ideal thermal emitter. Also, an optimistic effective filter transmittance, $\tau_g = 0.95$ was assumed.

There are several things to notice in figure 2. First of all, the maximum values for η_f and η_E occur when $E_b/kT_E \approx 4.0$. Therefore, if we limit the emitter temperature to 1500 °K, then $E_b \leq 0.52$ eV ($\lambda \geq 2.4$ μm). Second, in order for the filter TPV system, which uses an ideal black-body emitter, to be more efficient than the selective emitter system very low filter absorptivity, α_f, is required. Only if $\alpha_f < 0.1$ will $\eta_f > \eta_E$ for a selective emitter system with $\varepsilon_l/\varepsilon_b = \varepsilon_u/\varepsilon_b \geq 0.1$. Also, if $\alpha_f \leq 0.05$ and $\varepsilon_l/\varepsilon_b = \varepsilon_u/\varepsilon_b \leq 0.05$, then both η_E and η_f will be large.

The filter efficiency shown in figure 2 is for an ideal black-body emitter. If the thermal emitter is not a black-body, $\alpha_E < 1.0$ and there will be a significant reduction in η_f. This is illustrated in figure 3 where η_f is shown as a function of E_b/kT_E for several values of α_E with $\Delta E_b/E_b = 0.1$, $\alpha_f = 0.01$ and $\tau_g = 0.95$. Comparing figures 2 and 3 we see that if $\alpha_E \leq 0.95$ a large reduction in η_f occurs compared to the ideal case, $\alpha_E = 1$. If $\alpha_E \leq 0.9$, then η_f will be less than η_E, even for the optimistic filter properties, $\alpha_f = 0.01$ and $\tau_g = 0.95$.

From the results shown in figures 2 and 3, it appears that $\tau_g \geq 0.95$, $\alpha_f \leq 0.01$ and $\alpha_E \geq 0.9$ are required for the filter TPV system to have greater efficiency than the rare-earth oxide selective emitter, TPV system. These are severe requirements for a filter system.

3. THIN FILM SELECTIVE EMITTER

As figure 2 illustrates, the maximum selective emitter efficiency occurs at $E_b/kT_E \approx 4$. Therefore, if $T_E \leq 1500$K then $E_b \leq 0.52$ eV ($\lambda \geq 2.4$ μm) in order to obtain maximum efficiency. As a result, an efficient TPV system for this condition ($T_E \leq 1500$K) will require a PV material with a low bandgap energy E_g. If $\varepsilon_u \neq \varepsilon_l$, then the value of E_b/kT_E for maximum η_E will be shifted. From the results of Chubb (ref. 1) for $\varepsilon_l > \varepsilon_u$ then $E_b/kT_E < 4$, which means higher T_E for a given E_b. If $\varepsilon_u > \varepsilon_l$, then $E_b/kT_E > 4$, which means lower T_E for a given E_b.

Three rare-earth oxides have low emission band energy: neodymia Nd_2O_3, holmia, Ho_2O_3 and erbia, Er_2O_3. Characteristics of these three are listed in table I. Only Nd_2O_3 has the potential for reaching its maximum efficiency if T_E is limited to 1500K. However, Ho_2O_3 at $T_E = 1500K$ rather than 1800K (temperature for maximum η_E) results in a negligible reduction in η_E.

The mantle-type emitters of Nelson and Parent (refs. 4 and 5) have been used in combustion driven systems. However, other geometries that are more rugged and easily coupled to any thermal source have the potential for higher efficiency. Two of these concepts being investigated at the Lewis Research Center are the thin film selective emitter and the small-particle selective emitter (fig. 4). Both of these concepts can utilize a smaller characteristic dimension than the mantle-type emitter, which uses 5 to 10 μm diameter fibers. As already pointed out, Nelson and Parent (refs. 4 and 5) have demonstrated the importance of the small characteristic dimension for obtaining high efficiency.

So far, most of the work has been concentrated on the thin film selective emitter. An analysis using a modification of the three-band model described earlier which includes scattering has been completed. Results of that analysis are presented in reference 6. The important variables affecting the performance are the substrate emittance, $\varepsilon_{\nu s}$, the film optical depth,

$$K_\nu = (a_\nu + \sigma_\nu)d \tag{14}$$

where a_ν is the absorption coefficient, σ_ν is the scattering coefficient, d is the film thickness and Ω_ν the scattering albedo,

$$\Omega_\nu = \sigma_\nu/(a_\nu + \sigma_\nu) \tag{15}$$

As already mentioned the spectrum is modeled by three bands of constant properties; in the emission band ($E_b - \Delta E_b/2 \leq h\nu \leq E_b + \Delta E_b/2$), $K_\nu = K_b$, $\Omega_\nu = \Omega_b$ and $\varepsilon_{\nu s} = \varepsilon_{bs}$; below the emission band ($h\nu \leq E_b - \Delta E_b/2$), $K_\nu = K_l$, $\Omega_\nu = \Omega_l$ and $\varepsilon_{\nu s} = \varepsilon_{ls}$; above the emission band ($h\nu \geq E_b + \Delta E_b/2$) $K_\nu = K_u$ $\Omega_\nu = \Omega_u$ and $\varepsilon_{\nu s} = \varepsilon_{us}$. For given values of K, Ω and ε_s the emittance for each band can be calculated and used in equation (11) to calculate η_E. Similar to the results of figures 2 and 3, where ε_l, ε_b and ε_u are assumed to be constants, the maximum value of η_E occurs at $E_b/kT_E = 4$ when $\varepsilon_u = \varepsilon_l$.

Besides efficiency, the power emitted in the emission band is another important performance parameter for a thin-film selective emitter. Large emitted power/area translates into a low-mass space power system. The dimensionless power-density, p_E, from reference 6 is the following,

$$p_E = P_E/\sigma_{sb}T_E^4A_E = \varepsilon_b\, F(E_b/kT_E,\, \Delta E_b/E_b) \tag{16}$$

where, A_E is the selective emitter area, $F(E_b/kT_E, \Delta E_b/E_b)$ is given by equation (8) and σ_{sb} is the Stefan-Boltzmann constant.

The behavior of η_E and p_E as functions of the optical depth, K_b, are shown in figure 5 for no scattering and several values of the substrate emittance at the optimum value of $E_b/kT_E = 4$. It is also assumed that $\Delta E_b/E_b = 0.1$, $\varepsilon_{ls} = \varepsilon_{bs} = \varepsilon_{us}$ and that $K_l = K_u = 0.05K_b$. From Nelson and Parent's (refs. 4 and 5) results, it is expected that $0.01K_b \leq K_l \leq 0.1K_b$ and $0.01K_b \leq K_u \leq 0.1K_b$ for the rare-earth oxides. Also, $\Delta E_b/E_b = 0.1$ is representative of the rare-earth oxides. Figure 5 shows there is an optimum optical depth to attain maximum efficiency. However, as equation (16) shows, p_E depends on optical depth only through ε_b. Since ε_b increases monotonically with K_b, the power density, p_E, will also be a monotonically increasing function of K_b. Also, the substrate emittance, ε_s, will affect p_E only for small

optical depths. However, substrate emittance has a major effect on η_E. It appears that $\varepsilon_s > 0.1$ results in efficiencies that are too low to be of interest.

When scattering is included the magnitude of η_E and p_E are negligibly effected, (ref. 6). However, to obtain maximum η_E larger optical depths are required. Similarly, to obtain the same power density, p_E, with scattering as is obtained without scattering requires a larger optical depth.

To estimate the power density that can be expected from a rare-earth oxide selective emitter, assume that $K_b \approx 1.0$ for $\Omega = 0$. With $K_b \approx 1.0$ the efficiency will be less than maximum by only a small amount (fig. 5(b)) but p_E will be close to its maximum value. At $K_b = 1$ and $\Omega = 0$, figure 5(b) shows that $p_E \approx 0.058$. For Nd_2O_3 at $T_E = 1500K$ ($E_b/kT_E = 4$), $p_E = 0.058$ yields $P_E/A_E = 1.7$ w/cm^2. This compares with the solar flux at Earth orbit of 0.135 w/cm^2.

The important theoretical results for the solid-state rare-earth oxide selective emitters can be summarized as follows. For maximum efficiency the emitter temperature must satisfy $E_b/kT_E \approx 4$. If T_E is limited to 1500K, then only Ho_2O_3 and Nd_2O_3 have the potential for operation near maximum efficiency. For the thin-film selective emitter, the substrate emissivity, ε_s, is a critical parameter for determining efficiency. If $\varepsilon_s < 0.02$ then efficiencies greater than 0.5 are possible. Also, maximum η_E occurs at a single optical depth, $K_b = (a_b+\sigma_b)d_{opt.}$ Finally, although scattering causes a reduction in the emitted power, P_E, if scattering is present, larger optical depths can be used without greatly reducing the efficiency. As a result, P_E is expected to be nearly the same both with and without scattering.

Experimental work on the rare-earth oxide thin-film selective emitter is just beginning. As has already been pointed out, the film substrate must be of low emittance in order to obtain large η_E. In addition the substrate must have a high melting point. These two requirements limit the possible substrate materials. Copper is an excellent substrate candidate if $T_E < 1300K$. We have measured the total hemispherical emittance of highly polished copper for $600 \leq T \leq 1200K$. For this temperature range we find that $0.02 \leq \varepsilon_s \leq 0.04$. Thus we expect $\eta_E \geq 0.5$ (fig. 5) for Nd_2O_3 or Ho_2O_3 emitters.

We are currently applying the films of Nd_2O_3 and Ho_2O_3 on copper substrates using vacuum evaporation of the oxides. Heating of the compressed oxides powders has been done using an electron beam, however resistance heating of a tantalum boat containing the oxide powders will also be investigated. When satisfactory films have been deposited, their emissive properties will be measured with the aid of a high temperature furnace (maximum temperature of 1700 °C).

4. SPECTRALLY TUNED SOLAR CELLS

In principle, it is possible to select a semiconductor bandgap that will maximize cell efficiency for a particular wavelength of light. In practice it is difficult for the very short (i. e., less than 400 nanometers,), and the very long (greater than about 2.5 microns) wavelengths. In those cases, factors related to cell design, the quality of the bulk material, and cell interfaces and surfaces begin to become major problems. Figure 6 taken from reference 7, shows the calculated variation of efficiency with bandgap using monochromatic light; the wavelength of the incident light corresponds to the energy bandgap in each case. For this figure the cell temperature was assumed to be 25 °C. Under such conditions, solar cell efficiency will not have an optimum bandgap, as is the case for the solar spectrum. Instead it will asymptotically approach a limiting value of efficiency as shown in the figure. Gallium arsenide cells, for example, are predicted to have an efficiency exceeding 60%. Data are available at present only on GaAs cells designed for maximum efficiency in the solar spectrum. Even so, efficiencies exceeding 50% in these nonoptimized structures have been shown (ibid). Monochromatic illumination efficiencies of the GaSb cell, with a bandgap of 0.67 eV

have not yet been measured. Based on its performance as the bottom cell of a two-junction multiple bandgap solar cell, which has been shown to be as much as 8% in the full solar spectrum (ref. 8), the monochromatic cell efficiency can be expected to be in the vicinity of 30% in a real device.

Figure 7 contains a plot of solar cell bandgap as a function of lattice spacing for several III–V and II–VI compound semiconductors. As can be seen, there is no binary compound available that has a bandgap at 0.5 eV, which would be optimum for use with a neodymia emitter. Within the III–V materials, there are two possible options, both of which would use one of the existing III–V binary compound substrates: (1) develop one of several choices of lattice mismatched ternary compound cells, or (2) develop one of several lattice matched quaternary compound cells. Since it is desirable to limit the amount of lattice mismatch required in option 1 as much as possible, the choices for substrates are InP, GaSb, and InAs. These same substrates are also suitable for use with two of the quaternary compounds of primary interest for this application: $Ga_xIn_{1-x}As_yP$ and $Ga_xIn_{1-x}As_ySb$.

Although the use of quaternary compounds adds increased complexity to the growth of the cell structure, they have the advantage that a lattice matched compound with the desired bandgap can be found for each of the above substrates. Growth of the ternary materials is somewhat easier from a chemical and hydrodynamic point of view, but has the disadvantage of having to deal with the large density of crystalline defects caused by the mismatch in lattice parameters and thermal expansion coefficients.

5.0 RADIOISOTOPE THERMOPHOTOVOLTAIC ENERGY (RTPV) USING A SELECTIVE EMITTER

TPV energy conversion for space radioisotope power applications is of current research interest (refs. 9 to 11). Morgan, Horne and Brothers (ref. 9) present an analysis for the performance of a RTPV system using the United States Department of Energy radioisotope general purpose heat source (GPHS). Their system uses a gallium antimonide (GaSb) photovoltaic cell, which has a bandgap energy of 0.67 eV, so that it is suitable for low temperature use. This system does not utilize a selective emitter nor a bandpass filter. However, high reflectance ($\geq$0.9) is assumed to occur at the back side of the PV cell for photons with energy less than the bandgap energy. These photons are reflected back toward the emitter and can thus be absorbed by the thermal emitter. A maximum overall efficiency of 13% at $T_E = 1400K$ is predicted for this system (ref. 9). Morgan, Horne and Brothers (ref. 9) also mention that a proprietary modification of the isotope heat source will lead to efficiencies greater than 25%.

Nelson and Iles (ref. 10) discuss both rare-earth oxide selective emitters and low bandgap photovoltaic cells for use in TPV systems applicable for space power. They show spectral exittance data for the fibrous mantle emitters of several of the rare-earth oxides. Rose and Merryman (ref. 11) present a system study of a radioisotope thermoelectric power conversion system (RTG) using short half-life materials. For a man portable terrestrial unit they predict a power density of 25 W/kg using polonium (^{210}Po), which has a 0.38 year half-life. They conclude that a significant improvement in performance will occur if a more efficient energy conversion system, such as TPV, were used.

The lowest cost space RTPV system will use the existing U.S. Department of Energy GPHS thermal source, since the development costs for the thermal source will be avoided. As a result, consider the performance of a selective emitter RTPV system using the GPHS thermal source. Each block of the GPHS thermal source generates approximately 250 watts with the temperature limited to approximately 1200K. We considered the performance of a hypothetical RTPV system that uses a single block. Larger power output can be obtained by stacking blocks on top of each other.

Figure 8 shows the hypothetical, single block RTPV system. This configuration is similar to the RTPV system of reference 9. The GPHS block is surrounded by a structure that holds the PV cells and also provides cooling through a heat pipe radiator. To form the thin film selective emitter a low emittance substrate that will operate at 1200K, such as copper, with the desired rare-earth oxide deposited on it must be placed in contact with the GPHS block. Since the substrate can be very thin there should be negligible temperature difference between the GPHS block (1200K) and the rare-earth oxide emitter. The major design criteria is the emitter area required to maintain the GPHS block at 1200K. This emitting area, A_E, is determined by an energy balance on the GPHS block.

P_t = block output = 250w = total radiation output + thermal losses

$$P_t = \varepsilon_E \sigma_{sb} T_E^4 A_E + P_L = \varepsilon_E \sigma_{sb} T_E^4 A_E + (1 - \eta_{th}) P_t \tag{17}$$

$$A_E = \eta_{th} P_t / \varepsilon_E \sigma_{sb} T_E^4 \tag{18}$$

Where ε_E is the total emittance of the emitter, σ_{sb} is the Stefan-Boltzmann constant (σ_{sb} $= 5.67\times10^{-12}$ w/cm^2 K^4), η_{th} is the thermal efficiency (eq. (3)) and T_E is the emitter temperature. In equation (17) radiation back to the emitter, such as occurs in a filter system, is neglected. The total emittance of the emitter, ε_E, is obtained from equations (10) and (16),

$$\varepsilon_E = P_{rad} / \sigma_{sb} T_E^4 A_E = p_E / \eta_E \tag{19}$$

so that

$$A_E = \eta_{th} \eta_E P_t / p_E \sigma_{sb} T_E^4 \tag{20}$$

We assume the GPHS blocks will be stacked on top of each other to obtain the desired power level. Therefore, only the sides of the GPHS blocks are capable of radiating, ($A_B = 202$ cm^2). Therefore, our first design criteria is $A_E \leq A_B$. Since the system will be operating in the space vacuum, the only heat loss from the GPHS block will be conduction losses through any structure connecting the GPHS block to the surrounding PV cell structure. Therefore, we assume $\eta_{th} = 0.95$. Therefore, for $T_E = 1200$K and $P_t = 250$w equation (20) yields the following:

$$A_E = 21.3\ \eta_E / p_E \leq A_B = 202\ \text{cm}^2 \tag{21}$$

Thus the ratio η_E/p_E is limited, according to equation (21), to $\varepsilon_E = p_E/\eta_E \geq .11$.

Neodymia (Nd_2O_3) has the largest emitter efficiency at $T_E = 1200$K. Therefore, it was chosen for the emitter in our hypothetical RTPV system. For $T_E = 1200$K and a copper substrate with $\varepsilon_s = 0.037$ the emitter efficiency, η_E, and dimensionless power density, p_E, that satisfy equation (21) are shown in table II along with the other important parameters for the RTPV system. The maximum $\eta_E = 0.53$, however, this must be reduced to $\eta_E = 0.50$ in order to satisfy equation (21). The photovoltaic efficiency assumed, $\eta_{PV} = 0.3$, is for monochromator light at $E_g = 0.52$ eV, (fig. 6). Presently there is no PV cell with $E_g = 0.52$ eV. However, as already discussed, such a cell is feasible. With the efficiencies just discussed the overall system efficiency and electrical power output are the following (eq. (12)).

$$\eta_{Ts} = \eta_{th}\ \eta_E\ \eta_{PV} = 0.14 \tag{22a}$$

$$P_{EL} = \eta_{Ts} P_t = 35\ \text{watts} \tag{22b}$$

Now consider the mass of this hypothetical one GPHS block RTPV system. The major mass components are the GPHS block and the radiator necessary to reject the waste heat from the PV cells. The GPHS block has mass, $M_B = 1.45$ KG. The waste heat that must be rejected by the radiator, P_R, is the following (refer to fig. 1(b)).

$$P_R = P_t - P_{EL} - P_L$$

$$P_R = \eta_{th} (1 - \eta_E \eta_{PV}) P_t \tag{23a}$$

$$P_R = 202 \text{ watts} \tag{23b}$$

The radiator area, A_R, necessary to reject this waste heat in deep space where the sink temperature $T_\infty \rightarrow 0$, is the following.

$$A_R = P_R / \epsilon_R \sigma_{sb} T_R^4 \tag{24}$$

Assuming a radiator emittance, $\epsilon_R = 0.8$, and $T_R = T_{PV} = 298$ °K yields $A_R = 0.56$ m^2. To estimate the radiator mass we used a specific mass, $M_R/A_R = 3.6$ KG/m^2, which is the specific mass of a small heat pipe radiator operating at 300K proposed for use on the Space Station (ref. 12). The mass of the selective emitter, M_E, was approximated by the mass of a copper substrate of 0.08 cm thickness and area equal to A_E. The PV cell mass, which is nearly negligible, was approximated using a specific mass, $M_{PV}/A_{PV} = 0.65$ KG/m^2, taken from reference 13 for a GaAs cell module. We also assumed $A_{PV} = 2A_E$ to calculate M_{PV}. However, since M_{PV} is so small the A_{PV} approximation is not critical. To estimate the structure mass, M_{st}, that holds the PV cells and the GPHS block together, we assumed that $M_{st} = 0.1 (M_B + M_E + M_{PV})$.

The component masses are listed in table III. With these masses the specific power is 9.2 W/KG. The major mass component is the radiator. There are two ways to reduce the radiator mass. First of all, if the PV cells are transparent to the low energy photons ($E < E_g$), as are the GaSb cells used by Boeing (ref. 9), then the radiator heat load, P_R, will be reduced. Secondly, the PV cell operating temperature can be increased and thus T_R also. This will also reduce η_{PV} and thus increase P_R. However, the T_R^4 dependence of A_R will more than make up for the P_R increase so that A_R will be reduced. There will be some optimum T_R to yield the largest P_{EL}/M_T. Further system studies are required to find the maximum P_{EL}/M_T.

The proposed Boeing RTPV system uses 15 GPHS blocks. This system attains maximum performance, (efficiency = 0.13 and power density = 8.5 W/kg), at $T_E = 1400$K which is nearly identical with our result at $T_E = 1200$K. At $T_E = 1400$K our emitter efficiency and power density would be significantly increased. Also, to attain the 0.13 efficiency for the Boeing system, the low energy photons ($E < E_g$) must be reflected back to the emitter and reabsorbed. In our hypothetical selective emitter system this process is neglected. Therefore, if it were included larger efficiency would occur.

SUMMARY

TPV using a rare-earth oxide, thin-film selective emitter and a matched PV cell is an attractive energy conversion system for use with a radioisotope decay thermal energy source. We estimate an efficiency of 14% with a specific power of 9.2 w/KG for an operating temperature of 1200K. To achieve this performance requires two significant developments. First, a durable, rare-earth oxide thin film on a low emittance substrate must be developed. Secondly, a PV cell matched to the emission band of the emitter must be developed.

REFERENCES

1. Chubb, D.L.: Reappraisal of Solid Selective Emitters for Thermovoltaic Energy Conversion. IEEE Photovoltaic Specialists Conference, 21st, Vol. 2, IEEE, New York, 1990, pp. 1325–1333.

2. White, D.C.; and Schwartz, R.J.: PIN Structures for Controlled Spectrum Photovoltaic Converters. AGARD Colloquium, Gordon Breach Science, New York, 1967, pp. 897–922.

3. Guazzoni, G.E.: High Temperature Spectral Emittance of Oxides of Erbium, Samarium, Neodymium and Ytterbium, Appl. Spectr., vol. 26, no. 1, 1972, pp. 60–67.

4. Nelson, R.E.: Rare Earth Oxide TPV Emitters. International Power Sources Symposium, 32nd; Proceedings, Electromechanical Society, Pennington, NJ, 1986, pp. 95–100.

5. Parent, C.R.; and Nelson, R.E.: Thermophotovoltaic Energy Conversion with a Novel Rare Earth Oxide Emitter. IECEC '86; Proceedings of the Twenty-First Intersociety Energy Conversion Engineering Conference, Vol. 2, American Chemical Society, Washington, DC, 1986, pp. 1314–1317.

6. Chubb, D.L.; Flood, D.J.; and Lowe, R.A.: High Efficiency Thermal to Electric Energy Conversion Using Selective Emitters and Spectrally Tuned Solar Cells. NTSE–92 Nuclear Technologies for Space Exploration, D.M. Woodall, ed., American Nuclear Society, LaGrange Park, IL, 1992, pp. 281–293.

7. Olsen, L.C., et al.: GaAs Solar Cells for Laser Power Beaming. Proceedings of the 11th Space Photovoltaic Research and Technology Conference, NASA CP–3121, 1991, 9 p.

8. Avery, J.E., et al.: Lightweight Concentrator Module With 30% AM0 Efficient GaAs/GaSb Tandem Cells. IEEE Photovoltaic Specialists Conference, 21st, Vol. 2, IEEE, New York, 1990, pp. 1277–1281.

9. Morgan, M.D.; Horne, W.E.; and Brothers, P.R.: Radioisotope Thermophotovoltaic Power System Utilizing the GaSb IR Photovoltaic Cell. Proceedings of the Tenth Symposium Space Nuclear Power and Propulsion, AIP Conference Proceedings 271, M.S. El-Genk and M.D. Hoover, eds., American Institute of Physics, New York, 1993, pp. 313–318.

10. Nelson, R.E.; and Iles, P.A.: Possible Applications of Selective Emitters for Space Power. Presented at the Space Solar Power for Orbital and Lunar Missions, ASME/ASES/SOLTECH Joint Solar Energy Conference, Apr. 4-8, Washington, DC, 1993.

11. Rose, M.F.; and Merryman, S.A.: Small Lightweight RTG Power Systems Using Short Half-Life Materials. NTSE–92 Nuclear Technologies for Space Exploration, D.M. Woodall, ed., American Nuclear Society, LaGrange Park, IL, 1992, pp. 123–136.

12. Summary Report for Heat Pipe Radiator Concept for the Space Station Freedom. Prepared for NASA Johnson Space Center by OAA Corp., Greenbelt, MD, 1992.

13. Advanced Photovoltaic Solar Array Design, Final Technical Report 1986, Jet Propulsion Laboratory, Pasadena, CA, 1986.

TABLE I.—EMISSION BAND DATA FOR RARE-EARTH OXIDES

Emitter material	Emission band transition	Photon energy at center of emission band, E_b, eV	Photon wavelength at center of emission band, μm	Dimensionless bandwidth from $\Delta E_b/E_b$	Emitter temperature for maximum efficiency, $T_{E/opt} = 1/4\ eE_b/k$, K
Ytterbia Yb_2O_3	$^2F_{5/2} - {}^2F_{7/2}$	1.29	0.955	0.18	3740
Erbia Er_2O_3	$^4I_{13/2} - {}^4I_{15/2}$	0.827	1.5	0.05	2400
Holmia Ho_2O_3	$^5I_7 - {}^5I_8$	0.62	2.0	0.10	1800
Neodymia Nd_2O_3	$^4I_{13/2} - {}^4I_{9/2}$	0.52	2.4	0.15	1500

TABLE.—II PROPERTIES OF ND_2O_3 THIN FILM SELECTIVE EMITTER RTPV SYSTEM

Emitter temperature, K	1200
Emission band energy = PV cell bandgap energy, eV $E_b = E_g$	0.52
Dimensionless emission bandwidth, $\Delta E_b/E_b$	0.15
Film index of refraction	1.9
Below emission band optical depth, K_l	0.05 K_b
Above emission band optical depth, K_u	0.05 K_b
Emission band optical depth, K_b to yield $p_E/\eta_E = 0.11$	0.36
Reflectance at vacuum film interface	$\left(\frac{n_f - 1}{n_f + 1}\right)^2 = 0.096$
Copper substrate emittance, ε_s	0.037
Reflectance at film-substrate interface	$1 - \varepsilon_s = 0.96$
Emitter efficiency, η_E	0.50
Dimensionless emitter power density, p_E	0.057
PV cell efficiency, η_{PV}	0.3
PV cell temperature, K	298
Thermal efficiency, η_{th}	0.95

TABLE III.—MASS OF NEODYMIA SELECTIVE EMITTER RTPV SYSTEM USING A SINGLE GPHS BLOCK

Component	Mass, KG
GPHS block	$M_B = 1.45$
Nd_2O_3 selective emitter with 0.08 cm thick Cu substrate and $A_E = 202\ cm^2$	$M_E = 0.145$
PV cells with $A_{pv} = 2A_E\ M_{PV}/A_{PV} = 0.65\ ^{KG}/m^2$	$M_{PV} = 0.026$
Heat pipe radiator with $M_R/A_R = 3.6\ KG/m^2$	$M_R = 2.03$
Structure $M_{st} = 0.1(M_B + M_E + M_{PV})$	$M_{st} = 0.16$
Total mass, M_T	3.81
	$P_{EL}/M_T = 35/3.81 = 9.2\ w/KG$

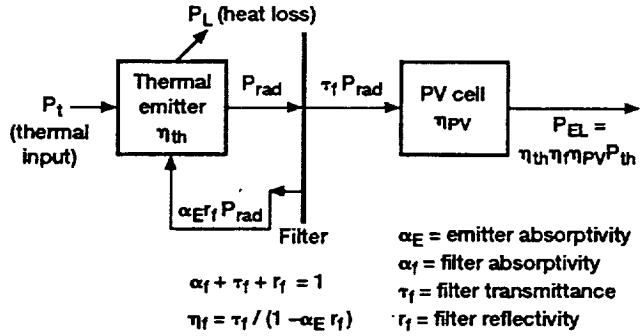

(a) Filter - thermal emitter TPV system.

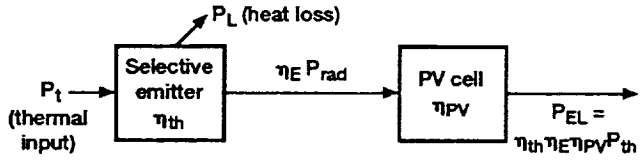

(b) Selective emitter TPV system.

Figure 1.—Schematic of TPV systems.

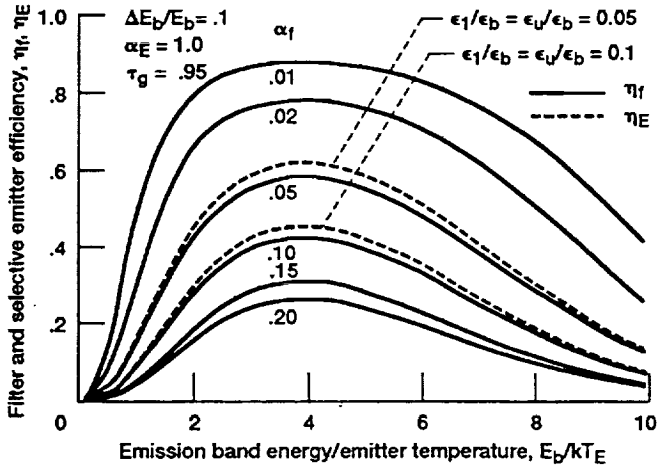

Figure 2.—Comparison of filter and selective emitter efficiency.

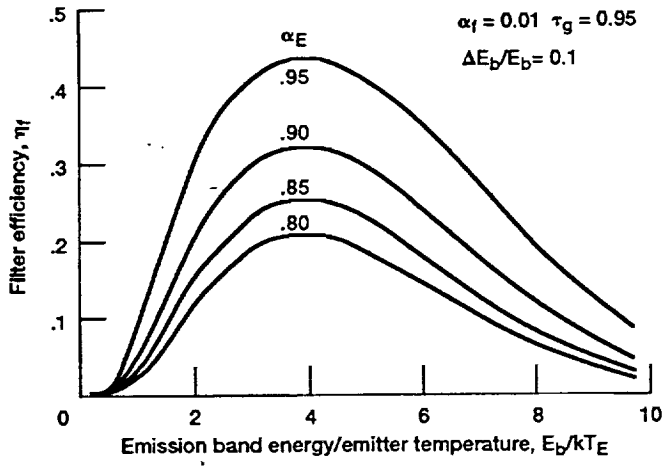

Figure 3.—Dependence of filter efficiency on thermal emitter absorptivity.

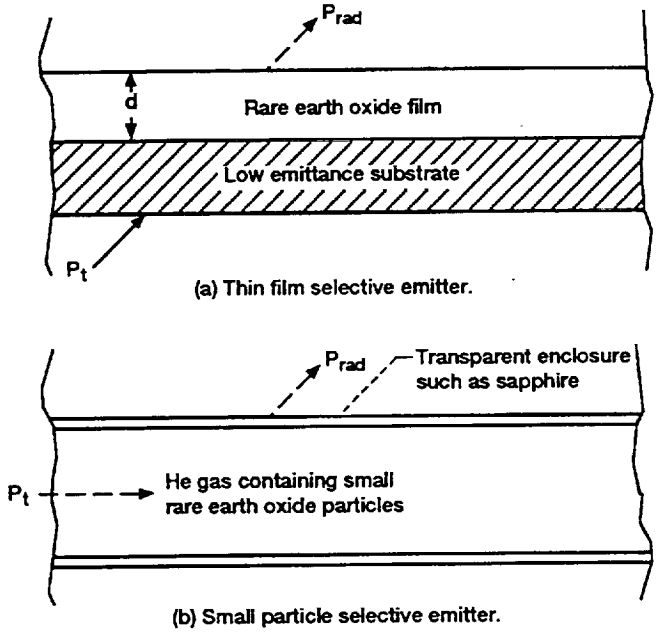

Figure 4.—Schematic of possible rare earth oxide selective emitters.

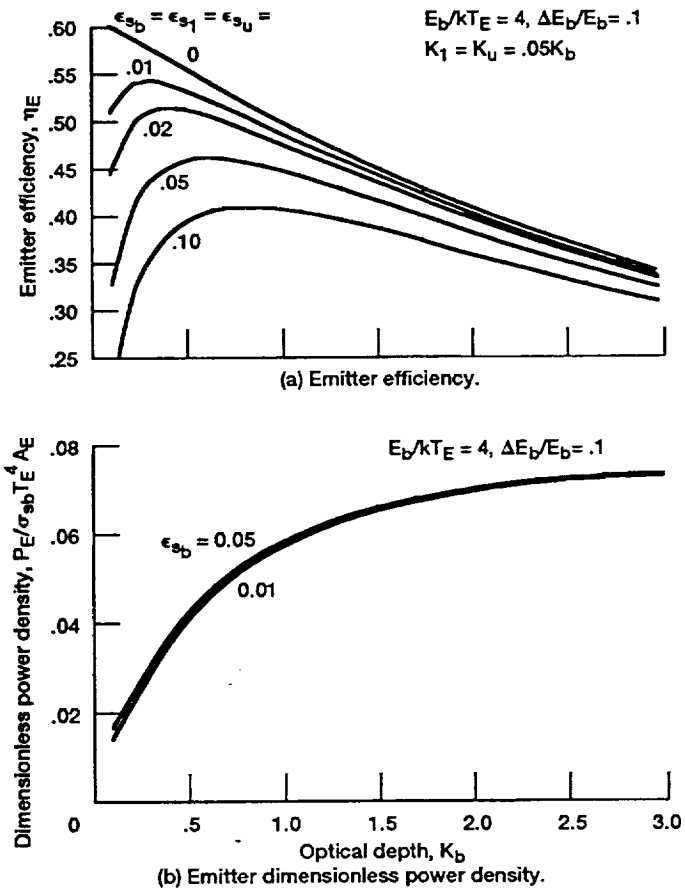

Figure 5.—Thin film emitter efficiency and power density for no scattering ($\Omega = 0$).

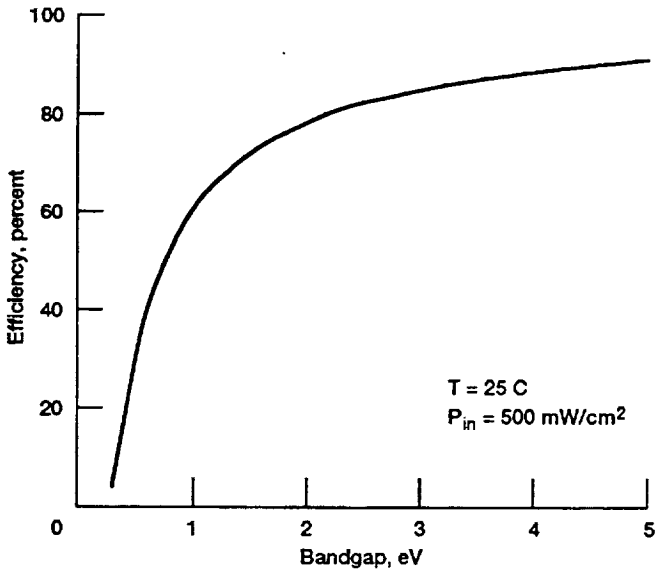

Figure 6.—Calculated efficiency for monochromatic cells coupled to laser light tuned to the cell material bandgap, and assuming an input power of 500 mW/cm^2.

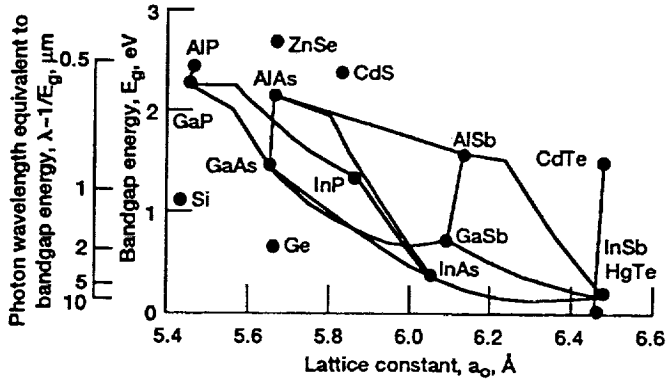

Figure 7.—Semiconductor bandgap energy as a function of lattice constant for various semiconductor materials.

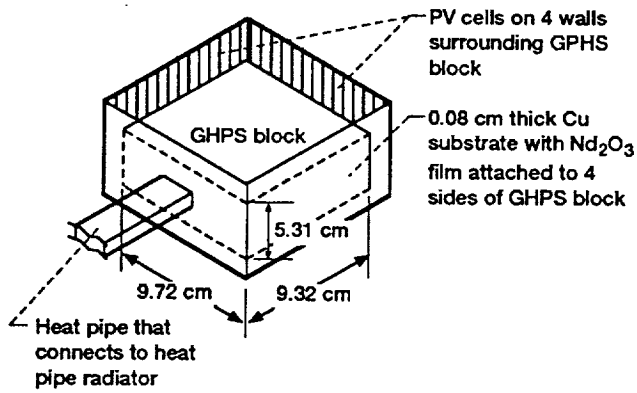

Figure 8.—Schematic drawing of thin-film selective emitter TPV system using a single GPHS block.

REPORT DOCUMENTATION PAGE

Form Approved
OMB No. 0704-0188

1. AGENCY USE ONLY (*Leave blank*)	2. REPORT DATE	3. REPORT TYPE AND DATES COVERED
	August 1993	Technical Memorandum

4. TITLE AND SUBTITLE

High Efficiency Direct Thermal To Electric Energy Conversion From Radioisotope Decay Using Selective Emitters and Spectrally Tuned Solar Cells

5. FUNDING NUMBERS

WU-506-41-11

6. AUTHOR(S)

Donald L. Chubb, Dennis J. Flood, and Roland A. Lowe

7. PERFORMING ORGANIZATION NAME(S) AND ADDRESS(ES)

National Aeronautics and Space Administration
Lewis Research Center
Cleveland, Ohio 44135-3191

8. PERFORMING ORGANIZATION REPORT NUMBER

E-7945

9. SPONSORING/MONITORING AGENCY NAME(S) AND ADDRESS(ES)

National Aeronautics and Space Administration
Washington, D.C. 20546-0001

10. SPONSORING/MONITORING AGENCY REPORT NUMBER

NASA TM-106227

11. SUPPLEMENTARY NOTES

Prepared for the Third European Space Power Conference cosponsored by the European Space Agency and Austrian Space Agency, Graz, Austria, August 23–27, 1993. Donald L. Chubb and Dennis J. Flood, NASA Lewis Research Center, Cleveland, Ohio 44135, and Roland A. Lowe, Cleveland State University, Cleveland, Ohio 44109. Responsible person, Donald L. Chubb, (216) 433–2242.

12a. DISTRIBUTION/AVAILABILITY STATEMENT

Unclassified - Unlimited
Subject Category 20

12b. DISTRIBUTION CODE

13. ABSTRACT ***(Maximum 200 words)***

Thermophotovoltaic (TPV) systems are attractive possibilities for direct thermal-to-electric energy conversion, but have typically required the use of black body radiators operating at high temperatures. Recent advances in both the understanding and performance of solid rare-earth oxide selective emitters make possible the use of TPV at temperatures as low as 1200K. Both selective emitter and filter system TPV systems are feasible. However, requirements on the filter system are severe in order to attain high efficiency. A thin-film of a rare-earth oxide is one method for producing an efficient, rugged selective emitter. An efficiency of 0.14 and power density of 9.2 W/KG at 1200K is calculated for a hypothetical thin-film neodymia (Nd_2O_3) selective emitter TPV system that uses radioisotope decay as the thermal energy source.

14. SUBJECT TERMS

Thermal photovoltaic (TPV); Selective emitters; Radioisotope thermal photovoltaic (TPV)

15. NUMBER OF PAGES

16

16. PRICE CODE

A03

17. SECURITY CLASSIFICATION OF REPORT	18. SECURITY CLASSIFICATION OF THIS PAGE	19. SECURITY CLASSIFICATION OF ABSTRACT	20. LIMITATION OF ABSTRACT
Unclassified	Unclassified	Unclassified	